The Company of **Biologists**

RESEARCH ARTICLE

The Mauthner cell in a fish with top-performance and yet flexibly tuned C-starts. I. Identification and comparative morphology

Peter Machnik, Kathrin Leupolz, Sabine Feyl, Wolfram Schulze and Stefan Schuster*

ABSTRACT

Archerfish use two powerful C-starts: one to escape threats, the other to secure prey that they have downed with a shot of water. The two C-starts are kinematically equivalent and variable in both phases, and the predictive C-starts – used in hunting – are adjusted in terms of the angle of turning and the final linear speed to where and when their prey will hit the water surface. Presently, nothing is known about the neural circuits that drive the archerfish C-starts. As the starting point for a neuroethological analysis, we first explored the presence and morphology of a pair of Mauthner cells, which are key cells in the teleost fast-start system. We show that archerfish have a typical Mauthner cell in each medullary hemisphere and that these send by far the largest axons down the spinal cord. Stimulation of the spinal cord caused short-latency all-or-none field potentials that could be detected even at the surface of the medulla and that had the Mauthner cell as its only source. The archerfish's Mauthner cell is remarkably similar morphologically to that of equally sized goldfish, except that the archerfish's ventral dendrite is slightly longer and its lateral dendrite thinner. Our data provide the necessary starting point for the dissection of the archerfish fast-start system and of any role potentially played by its Mauthner cell in the two C-start manoeuvres. Moreover, they do not support the recently expressed view that Mauthner cells should be reduced in animals with highly variable fast-start manoeuvres.

KEY WORDS: Escape response, Reticulospinal system, Speed–accuracy, Fast start, Neuroethology

INTRODUCTION

The life-saving escape C-starts of teleost fish are among the fastest responses known in the animal kingdom (Eaton, 1984; Sillar et al., 2016). Driven by a relatively small reticulospinal network (Zottoli, 1977; Eaton et al., 1981; Korn and Faber, 1996; Kohashi and Oda, 2008; Neki et al., 2014; Dunn et al., 2016) of a few hundred neurons (Faber et al., 1989; Fetcho, 1991, 1992; Zottoli and Faber, 2000), they rapidly turn the fish away from a zone of danger. Within this network, a pair of large identified neurons, the so-called Mauthner cells, usually takes a unique position, with a size and axon diameter that by far exceeds those of any other reticulospinal neuron (e.g. Zottoli, 1978; Zottoli and Faber, 2000; Korn and Faber, 2005; Sillar, 2009). In the intact escape system of goldfish, the firing of one spike in one Mauthner cell causes a rapid C-shaped bending to the contralateral site and any rapid C-start involves a spike in one of the

two Mauthner cells (Zottoli, 1977). Several studies have been able to directly link intracellularly recorded responses of the goldfish Mauthner neuron under *in vivo* conditions to behaviourally measured changes that occurred during sensory gating, temperature acclimatisation or learning (Oda et al., 1998; Preuss and Faber, 2003; Neumeister et al., 2008; Szabo et al., 2008; Preuss et al., 2006). Nevertheless, the role of the Mauthner cell and reasons for its absence in some fish (Stefanelli, 1951, 1980) and in terrestrial vertebrates (Zottoli, 1978) are still under debate. Earlier findings suggested that removal of the Mauthner cell had only a small effect on escapes (Kimmel et al., 1980; Eaton et al., 1982; DiDomenico et al., 1988), which led to the concept that Mauthner cells do not drive the C-start, but are needed to shut off other, potentially conflicting motor behaviours (Eaton et al., 1995). However, when an important class of inhibitory neurons was left intact, a clear effect of Mauthner cell ablation on response probability and latency could be seen (Zottoli et al., 1999). Work in zebrafish larvae showed that ablating the Mauthner cell together with its two serially homologous cells (called MiD2cm and MiD3cm) abolishes the ability to execute rapid short-latency C-starts (Liu and Fetcho, 1999), so that these six cells, the so-called Mauthner series, would seem to play a prominent role in driving urgent C-starts. A recent study simultaneously monitored the behavioural performance in zebrafish larvae during the first bending phase of the C-start as well as activity within the reticulospinal network. This study found that the Mauthner cell was always active in the fastest, but stereotypical C-starts, but never in slower, but graded and variable C-starts (Bhattacharyya et al., 2017), which fits the often-expressed view that the rapid Mauthner-driven escape C-starts are 'stereotyped' and 'robust' escape 'reflexes' (e.g. Zottoli, 1977; Dunn et al., 2016). In the light of Foreman and Eaton's (1993) direction change concept, the findings would suggest that variability is possible when the network is active, but absent when the Mauthner cell is recruited. Based on their findings, Bhattacharyya et al. (2017) suggested an evolutionary scenario in which the giant Mauthner cells of fish and some amphibians were no longer useful for initiating the more flexible behaviours of land-living vertebrates and were consequently reduced.

In this context, it would be particularly interesting to probe for the presence of any typical Mauthner cells in the fast-start system of archerfish. Archerfish show rapid and powerful C-starts as a part of their hunting behaviour (Wöhl and Schuster, 2007; Schlegel and Schuster, 2008; Rischawy et al., 2015). These predictive C-starts are kinematically equivalent to the archerfish escape C-starts (Fig. 1). Both C-starts are variable in their two major phases, the bending phase, in which the fish takes the shape of a letter C, and the subsequent straightening phase, in which it accelerates by pushing water backwards (Wöhl and Schuster, 2007). In the predictive starts, the first bending phase largely determines the turn angle, whereas the subsequent straightening phase largely determines take-off speed (Wöhl and Schuster, 2007; Reinel and Schuster, 2014). Both phases are matched to the initial motion of ballistically falling prey

Department of Animal Physiology, University of Bayreuth, D-95440 Bayreuth, Germany.

*Author for correspondence (stefan.schuster@uni-bayreuth.de)
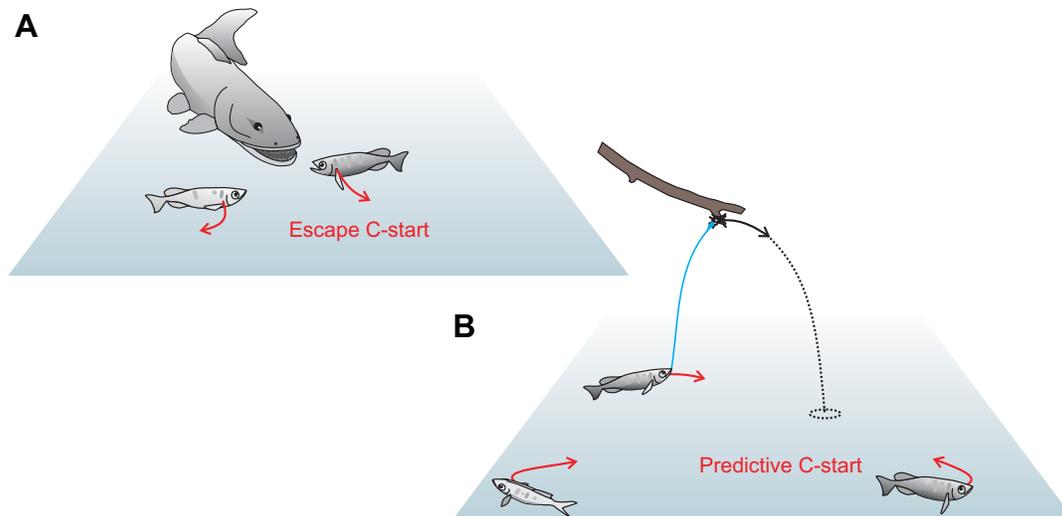
S.S., 0000-0003-2828-9355

Fig. 1. The two types of high-performance rapid fast-starts in archerfish. Archerfish perform two types of C-starts: escape and predictive. They are kinematically identical and are among the most powerful (peak angular acceleration >450,000 deg s^{-2}, linear acceleration up to 12 times gravitational acceleration; Wöhl and Schuster, 2007) known in teleost fish. Escape C-starts are produced in response to threats (A) and predictive C-starts are used as a part of their hunting behaviour (B). In contrast to the escape responses, both phases of the predictive C-starts are precisely adjusted so that the fish will end its C-start oriented towards the later point of prey impact (Rossel et al., 2002; Schlegel and Schuster, 2008) and at a linear speed that, when maintained, would make the fish arrive at the point of catch just in time and with minimal travel costs (Wöhl and Schuster, 2006; Reinel and Schuster, 2014). In this and the accompanying paper (Machnik et al., 2018), we establish whether a teleost-typical Mauthner cell is part of the archerfish's fast-start system. This is the necessary first step in a neuroethological analysis of the two C-starts, but also is a test of the recent suggestion that Mauthner cells should be less important in animals with variable and fine-tuned fast-start manoeuvres.

(e.g. Reinel and Schuster, 2014, 2016). If the giant Mauthner neurons were not useful for driving more variable C-starts, then one would expect them to be reduced or even absent in adult archerfish. In contrast, if they were used, the views of Bhattacharyya et al. (2017) and others would predict amendments needed to attain the flexibility of the archerfish starts. Hence, and regardless whether the Mauthner cells (if they exist) are involved in any of the archerfish's C-starts, one would expect to find in archerfish differences relative to a 'teleost-typical' Mauthner cell like that of goldfish – provided the view is correct that 'typical' Mauthner cells are not useful to initiate variable starts. We therefore decided to critically probe for the existence and structural properties of any neuron with Mauthner-like morphology in archerfish, using equally sized goldfish for direct comparison. Moreover, if we could find a Mauthner neuron, this would provide an extremely valuable, if not essential, starting point for a more detailed characterisation of the archerfish fast-start system (in ways achieved in goldfish; Neki et al., 2014). Furthermore, it would be the basis for a direct analysis of whether the Mauthner cell is involved in triggering either of the two archerfish C-starts.

MATERIALS AND METHODS
Experimental animals
We used banded archerfish [*Toxotes jaculatrix* (Pallas 1767), Perciformes] of either sex with 7–8 cm standard length. The fish were obtained commercially from an authorised specialist retailer (Aquarium Glaser GmbH, Rodgau, Germany). They were kept in groups of up to 20 individuals in tanks (120×50×50 cm) with brackish water (water conductivity: 3.25 mS cm^{-1}) at 26°C and on a 12 h:12 h light:dark regime for at least 12 weeks prior to experimentation. Water of the same quality was used in the electrophysiological recording chamber. The fish were fed with cichlid sticks (sera GmbH, Heinsberg, Germany), defrosted *Artemia* and red mosquito larvae. We only used healthy animals with natural

behaviour and no signs of injury or disease. Additionally, we used goldfish [*Carassius auratus* (Linnaeus 1758), Cypriniformes] of equal size for a direct comparison of various morphological aspects of the archerfish Mauthner cell with that of goldfish. Goldfish were kept in freshwater (water conductivity: 0.30 mS cm^{-1}) at 22°C. Animal care procedures, surgical procedures and experiments were in accordance with all relevant guidelines and regulations of the German animal protection law and explicitly approved by state councils.

Anaesthesia and surgical procedure
Similar procedures were used for archerfish and goldfish. Prior to surgery, the experimental animal was anaesthetised (in water from its home tank) for at least 30 min using 0.4 ml l^{-1} of the general anaesthetic 2-phenoxyethanol (2-PE; Sigma-Aldrich, Steinheim, Germany). The choice of 2-PE (and not the customary MS-222) was crucial for the accompanying paper (Machnik et al., 2018). As an additional local surface anaesthetic, we applied 20% benzocaine gel (Anbesol maximum strength gel, Pfizer Inc., Kings Mountain, NC, USA) to the incision sites on the skin (see below). The fish was then placed in the recording chamber, where ventilation was established with aerated water (70–100 ml min^{-1}). To maintain anaesthesia throughout the experiment, ventilation water also contained 0.4 ml l^{-1} 2-PE. The spinal column was exposed at the level of the beginning of the dorsal fin (2.8–3.0 cm caudal from the level of the Mauthner cell) using a scalpel, a sharp curette and splinter tweezers. A bipolar stimulation electrode then was placed on the exposed spinal cord and electrical stimuli (see below) were applied to cause twitching of the experimental animal (e.g. Faber and Korn, 1978; Zottoli, 1978) and thus to confirm activation of neurons in the spinal cord. Subsequently, the fish was immobilised by intramuscular injection of d-tubocurarine (Sigma-Aldrich; 1 µg g^{-1} body mass). To expose the brain, we opened the cranium from above using a bone rongeur. To obtain access to the

medulla, the cerebellum was carefully lifted upward and kept in a lifted position using a strip of wet filter paper. After removing the meninges, we positioned a recording electrode on the surface of the medulla and started searching for spots at which the field potential was maximal – potentially indicative of Mauthner-like neurons. During this search, the spinal cord was stimulated electrically (rate: 2 Hz; pulse duration: 10 µs; pulse amplitude: usually between 8 and 12 V, but in some experiments up to 60 V) using a constant-voltage isolated stimulator (DS2A2 – MkII, Digitimer Ltd, Hertfordshire, UK).

Electrophysiological measurements
We used a bridge-mode amplifier (BA-01X, npi electronic GmbH, Tamm, Germany) in current-clamp mode for electrophysiological measurements with sharp electrodes. Recording electrodes (4–7 MΩ) were pulled from 3 mm glass (G-3, Narishige Scientific Instrument Lab, Tokyo, Japan) using a vertical electrode puller (PE-22, Narishige International Limited, London, UK) and were filled with 5 mol l^{-1} potassium acetate. A motorised micromanipulator (MP-285, Sutter Instrument, Novato, CA, USA) was used to move and position the recording electrode. Recordings were filtered (Hum Bug Noise Eliminator, Quest Scientific, North Vancouver, BC, Canada) and digitised using an A/D converter (Micro1401, Cambridge Electronic Design Ltd, Cambridge, UK) at 50 kHz sampling rate and the acquisition software package Spike2 (version 6; Cambridge Electronic Design Ltd). Spike2 was also used for data analysis.

Morphological examination
To examine the morphology of cells penetrated at the focus points of the field potential, we filled the electrodes with Neurobiotin™ tracer (BIOZOL Diagnostica, Eching, Germany) in 1 mol l^{-1} potassium chloride. The tracer was injected into the soma iontophoretically (e.g. Smith and Pereda, 2003). To avoid damaged cells being included in our characterisation, we only processed cells that could still be activated by spinal cord stimuli after tracer injection. If this was the case, we extracted the brain and fixed it using 4% paraformaldehyde solution at 4°C. This approach is suitable because a craniotomy was required to access the medulla for intracellular Mauthner cell labelling. Once labelling was finished, the added paraformaldehyde quickly spread within the brain. Because we initially applied transcardial fixative perfusion, we could directly compare slices obtained with the two methods. The absence of any advantage led us to discard the perfusion method here. The fixed brain was subsequently sliced (slice thickness 40–80 µm for coronal slices, 100 µm for horizontal slices) using a vibrational microtome (VT1200 S, Leica Microsystems, Wetzlar, Germany), washed and incubated with Streptavidin-Cy3 (Sigma-Aldrich) in PBX (PBS+0.3% Triton™ X-100; Sigma-Aldrich). Streptavidin specifically binds to the Neurobiotin™ tracer (Huang et al., 1992). We examined the slices using a fluorescence optical microscope (Axio Scope.A1, Carl Zeiss Microscopy, Jena, Germany). If parts of a fluorescent cell were found in consecutive slices, we reconstructed the cell using the software package Adobe Photoshop CS3 Extended (Adobe Systems Inc., San Jose, CA, USA).

Statistical analyses
Statistical tests were run using the software package GraphPad Prism 5.0f (GraphPad Software, Inc., La Jolla, CA, USA). Gaussian distribution was checked with Shapiro–Wilk tests. All tests were two-tailed with a significance level of α=0.05. Means±s.e.m. are

given; N and n denote the number of animals and measurements, respectively. The 3D map and the heat map were constructed in SigmaPlot 11.0 (Systat, Inc., Erkrath, Germany). To compare dendrite diameters, we took systematic measurements in steps of 50 µm along the two major dendrites, starting with the broadest point of the soma. To compare values in regard to the measuring position, we used the Wilcoxon matched-pairs signed-rank test. This analysis involved N=4 archerfish and N=4 goldfish.

RESULTS
A short-latency all-or-none field potential in the archerfish medulla
Spinal cord stimulation caused a negative field potential in the archerfish medulla that could be indicative of Mauthner-like neurons. The field potential could readily be picked up at the surface of the medulla (-0.24 ± 0.01 mV; N=10). When we decreased the strength of spinal cord stimulation step by step, the field potential did not decrease gradually, but at some point vanished abruptly. It also came back abruptly to its previous level, when stimulus strength was increased again. This important feature was generally observed at all spots within the medullae of all 30 archerfish. The field potentials were thus clearly of an all-or-none character and their amplitude was fixed for any location within the medulla. Fig. 2 illustrates these properties for three points in the medulla of an archerfish. For each point, Fig. 2 reports measurements of the extracellular field potentials caused by spinal cord stimuli of largely varying strength from 5 to 60 V. Most remarkable is the independence – over the full range of appropriate stimuli – of the amplitude of the field potentials at any given location from the amplitude of the spinal cord stimuli (Fig. 2B; linear regression analysis; $r^2 \leq 0.16$, $P \geq 0.22$ in all plots). Furthermore, the rising time of the potentials from onset to their extreme value was also always short (0.45 ± 0.01 ms for spinal cord stimuli between 8 and 12 V, measured at the medullary surface; N=10) and did not increase even when the amplitude of spinal cord stimulation was strongly increased (Fig. 2C; linear regression analysis; $r^2 \leq 0.13$, $P \geq 0.28$ in all plots). Moreover, rising time did not correlate with the amplitude of the field potential (correlation analysis; $r^2 \leq 0.17$, $P \geq 0.21$). These findings clearly illustrate the all-or-none nature of the field potential as opposed to a potential caused by the activity of several units. In the latter case, stronger spinal cord stimuli should activate more units, which should cause the amplitude and/or duration of the rising phase to increase. Fig. 2D draws attention to further typical aspects of the all-or-none potentials. First, they arose with remarkably short latency of less than 0.3 ms after the spinal cord stimuli (0.27 ± 0.004 ms for spinal cord stimuli between 8 and 12 V, measured at the medullary surface; N=10). Second, latency depended on the amplitude of the spinal cord stimuli, but also on the recording position. The effect of amplitude is apparent [and due to our use of a fixed (arbitrary) threshold to define the onset of the field potential], but the dependence on position is an interesting additional property of the all-or-none potential.

The field potential has only one source per medullary hemisphere
The all-or-none characteristics speak against the field potential being produced by many independent units with different stimulation thresholds. Nevertheless, it could still be caused by several coupled units, distributed all over the medulla, but co-activated by the spinal cord stimuli. We therefore explored in detail the spatial distribution of the field potential within the archerfish
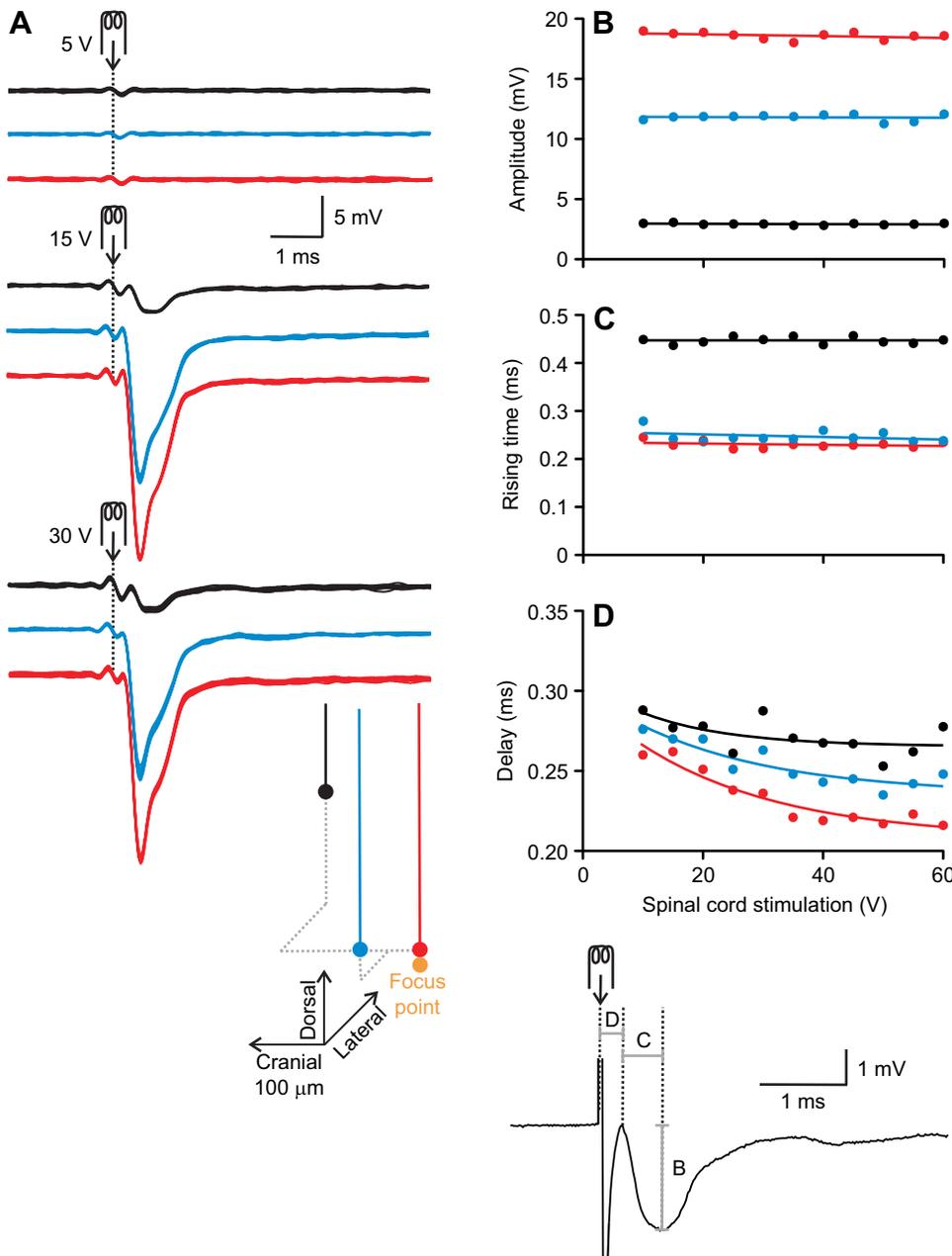
Fig. 2. A short-latency all-or-none field potential in the archerfish medulla. Stimulating the spinal cord above a critical voltage caused a typical negative field potential in the archerfish medulla. (A) Fifteen superimposed recordings at three precisely set positions (see inset; see Results for definition of focus point) in the medulla of an archerfish. Spinal cord stimuli were either below (5 V) or above threshold (15 and 30 V). Note the perfect alignment of each of the 15 recordings made at each given position. The inset shows the recording position in relation to a focus point that will be discussed later (Fig. 3). (B–D) Detailed analysis of the dependence of amplitude (B), rising time (C) and delay (D) of the field potential (illustrated in the inset) on the amplitude of spinal cord stimuli for the three positions. At each circle, 100 measurements were taken that all showed no conspicuous variation (as illustrated in the traces shown in A). Field potential amplitude (B) and rising time (C) were remarkably independent of stimulation strength (linear regression analysis; $P \geq 0.22$ in all cases), demonstrating the all-or-none nature of the field potentials. Delays (D) were always below 0.3 ms.

medulla. To find one or several spots (focus points) where the field potential was maximal, we scanned the medullae of 30 archerfish in their entire range [i.e. depth from 0 (at the medullar surface) to 1800 µm; distance from the fourth ventricle in the caudal direction: 0 to 850 µm] and also explored the medullae along various paths up to 600 µm lateral from the midline. Scanning was done so as to exclude any bias to one particular focus point. To illustrate the search procedure, Fig. 3A–C shows three search paths that each led to a focus point. Each search started at the centre of the entrance to the fourth ventricle. The recording electrode was then moved caudally and/or laterally, initially in steps of 50 µm. When we detected a change in the field potential from one position to the next that was larger than 2 mV, we decreased the step size. Regardless of the particular path chosen, we always found one and only one spot per medullary hemisphere in which the magnitude of the field was maximal. In the 30 fish of equal size, the average position of this spot could be determined quite accurately. It was 244.7±17.2 µm

caudal from the fourth ventricle, 312.0±9.4 µm lateral from the midline and 995.3±26.6 µm under the surface of the medulla. The magnitude of the field potential at these spots ranged from 21.7 to 26.9 mV. Fig. 3D,E shows the positions of all 30 focus points in archerfish and in goldfish relative to the major landmarks in the medulla (midline and fourth ventricle). We directly report absolute sizes, because the dimensions of the medullae were not significantly different between the goldfish and archerfish used here (difference between archerfish and goldfish in length and width of the medulla: unpaired *t*-tests, $P \geq 0.3$ for both measures; depth of the medulla: Mann–Whitney test, $P=0.6$). Fig. 3 thus can be helpful for indicating in which range to expect a focus point. Note that the degree of variation was similar in the equally sized medullae of archerfish and goldfish. In goldfish, the negative spike focus was 386.3±18.2 µm caudal from the fourth ventricle, 395.8±9.3 µm lateral from the midline and deeper in the medulla, at 1266.0±24.5 µm from its surface. The magnitude of the field potential at these spots, however,
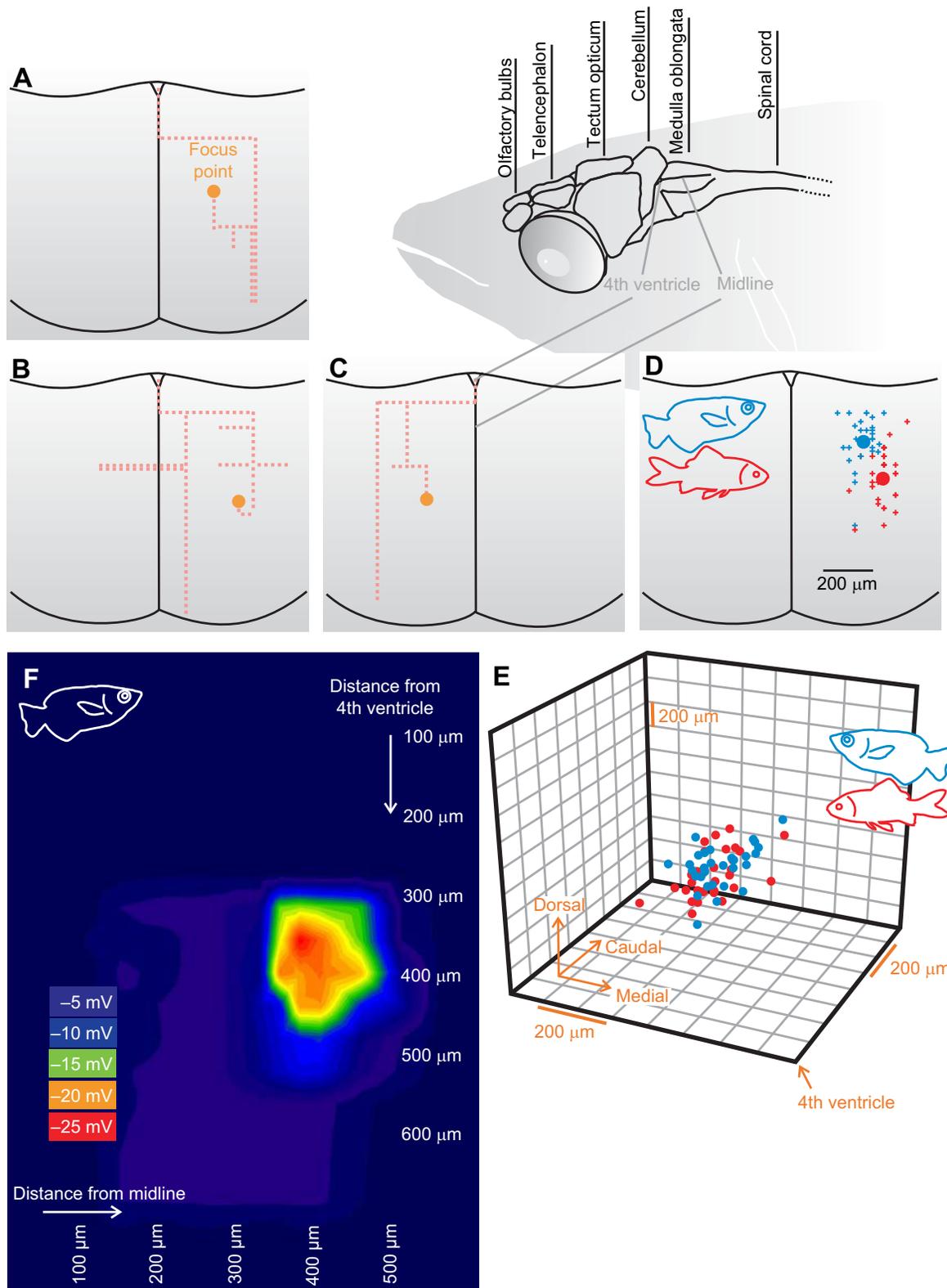
Fig. 3. A single source in each hemisphere of the archerfish medulla accounts for the all-or-none potential. (A–C) Schematic illustration of the archerfish medulla and three representative approach paths used to identify spots in the medulla at which the all-or-none field was maximal. The respective focus points are marked by orange circles. (D,E) Distribution of focus points in all archerfish (blue, N=30 fish) and goldfish (red, N=30) examined. Maps report position relative to the fourth ventricle and midline of the right half of the medulla. Large circles in D indicate the averaged focus point position. (F) Example of a detailed map of the magnitude of the extracellular negative all-or-none field potential within the horizontal plane of the right medullary hemisphere. Note that the recordings were taken after the centre had been identified so that the specific distance from the fourth ventricle and from the midline could be determined. To generate the map, we took 336 sampling points in the entire right medullary hemisphere. The distance between sampling points ranged from 20 to 100 μm depending on the steepness of the gradient of the field potential.

was similar to what we found in archerfish and ranged from 19.1 to 25.4 mV.

Fig. 3F illustrates a typical distribution of the magnitude of the negative all-or-none field potential around a focus point. In this example (but not in the search that had identified the focus point in the first place), mapping started at the entrance to the fourth ventricle and extended 800 μm caudally and 600 μm laterally from this point. Step size was between 20 and 100 μm in the horizontal plane, with smaller steps made when the gradient of the field potential increased. In the vertical plane, we traversed the brain to the depth that showed the local field potential maximum. Both dorsally and ventrally, the field potentials were smaller. In summary, our mapping of the distribution of the field potential suggests that it is caused by a single point-type source.

However, it was still possible that the field was generated by two co-activated point sources that we were unable to separate in our scans. To address this concern, we analysed the decay characteristics of the field potential (Fig. 4). Suppose that the field was caused by two very close co-activated sources, which are a distance D apart. Then the vertical decay of the field should be better described by a two-source Coulomb potential of the form $V_{C2}(d)=a[1/d+1/(d+D)]$ rather than by one with one source, $V_{C1}(d)=a/d$ (where V is voltage, d is vertical distance and a is a constant). However, the single-source decay fits the course better than the optimal two-source model (with inferred source distance $D=12$ μm). One could still object that the analysis rests on the assumption of a simple Coulomb field. Clearly, such a field does not adequately describe the data and does not

account for the finite initial slope at the focus point (0.73 mV μm^{-1} in Fig. 4A). In fact, an exponential course $V(d)=A\exp(-d/\lambda)$ with a decay constant of $\lambda=38$ μm describes the vertical decay of the field far better ($r^2=0.99$) than both a one-source and a two-source Coulomb potential (V_{C1} with $r^2=0.35$, and V_{C2} with $r^2=0.33$). However, with the exponential decay the fits were also not better with two sources.

Hence, we conclude that there is only one source of the field potential per medullary hemisphere. At each focus point, we could penetrate a neuron that fired a single action potential after each spinal cord stimulation (Fig. 4B). Furthermore, the latency from spinal cord stimulation to action potential was always (in 30 of 30 cases) indistinguishable from the latency from spinal cord stimulation to the onset of the extracellular field potential (paired t-test; $P=0.85$). We stained six of the neurons penetrated this way in order to analyse their position within the medulla, the course of their axons and to study their rough morphology. By also processing six Mauthner neurons in goldfish of similar size using the very same techniques as in archerfish, we hoped to be able to see whether we had identified the archerfish Mauthner cells.

The archerfish Mauthner neuron

The criteria of Zottoli (1978) clearly allow us to say that the stained neurons were the archerfish Mauthner cells. These criteria demand that a typical teleost Mauthner cell has (i) a large soma, (ii) two large primary dendrites, (iii) an axon that decussates and has (iv) the largest diameter of any axon in the spinal cord. Additionally, the
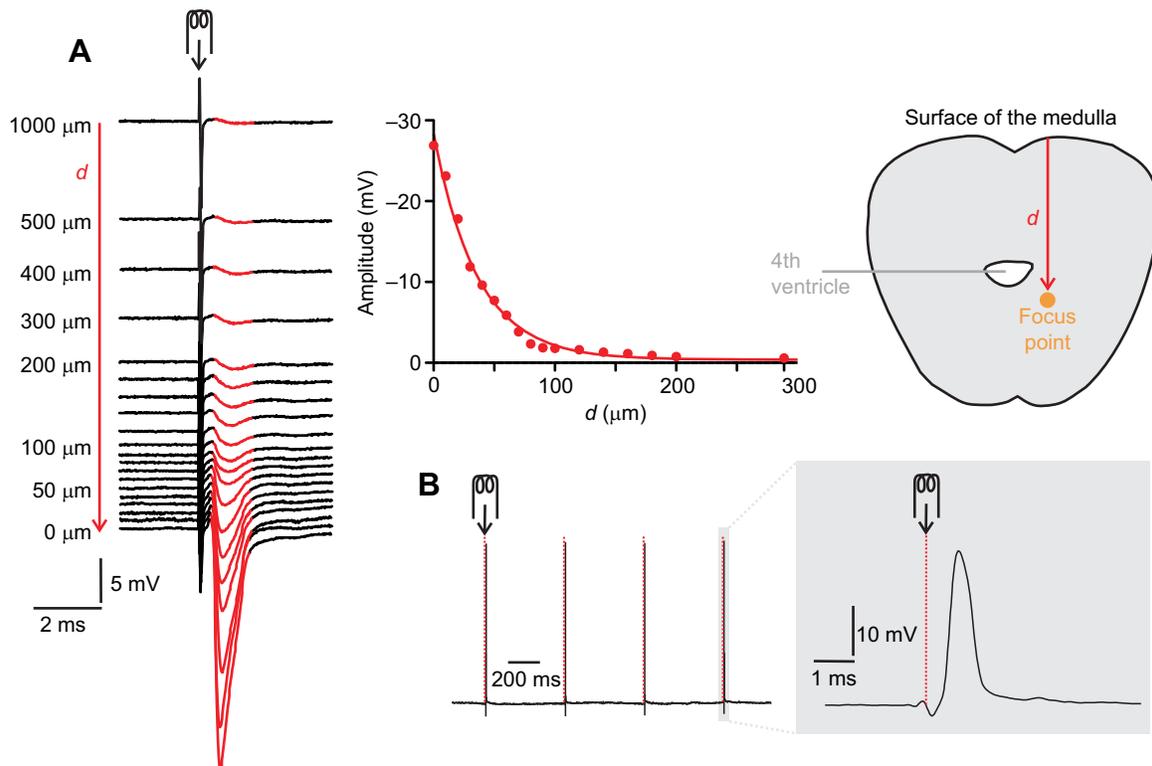

Fig. 4. Analysis of the vertical decay suggests a point source. (A) The extracellular field potential – induced by suprathreshold electrical spinal cord stimuli – could be detected at the surface of the medulla of archerfish. The amplitude of its negative peak (red) is shown during a direct vertical approach toward the focus point. In the diagram, the focus point is assigned a distance (d) of 0 μm, the origin of the y-axis. Its decay is best described by a simple exponential fit with (vertical) decay constant 38 μm and initial slope −0.73 mV μm^{-1}. (B) In this example, advancing the electrode beyond the focus point (with potential −26.9 mV) caused penetration of the cell shown in Fig. 6A. Suprathreshold spinal cord stimulation caused consistent low-latency single action potentials in this cell, the latency of which was identical to that of the field potentials and the shape of which – with no observable hyperpolarisation and (apparent) low amplitude – is typical for a Mauthner cell.
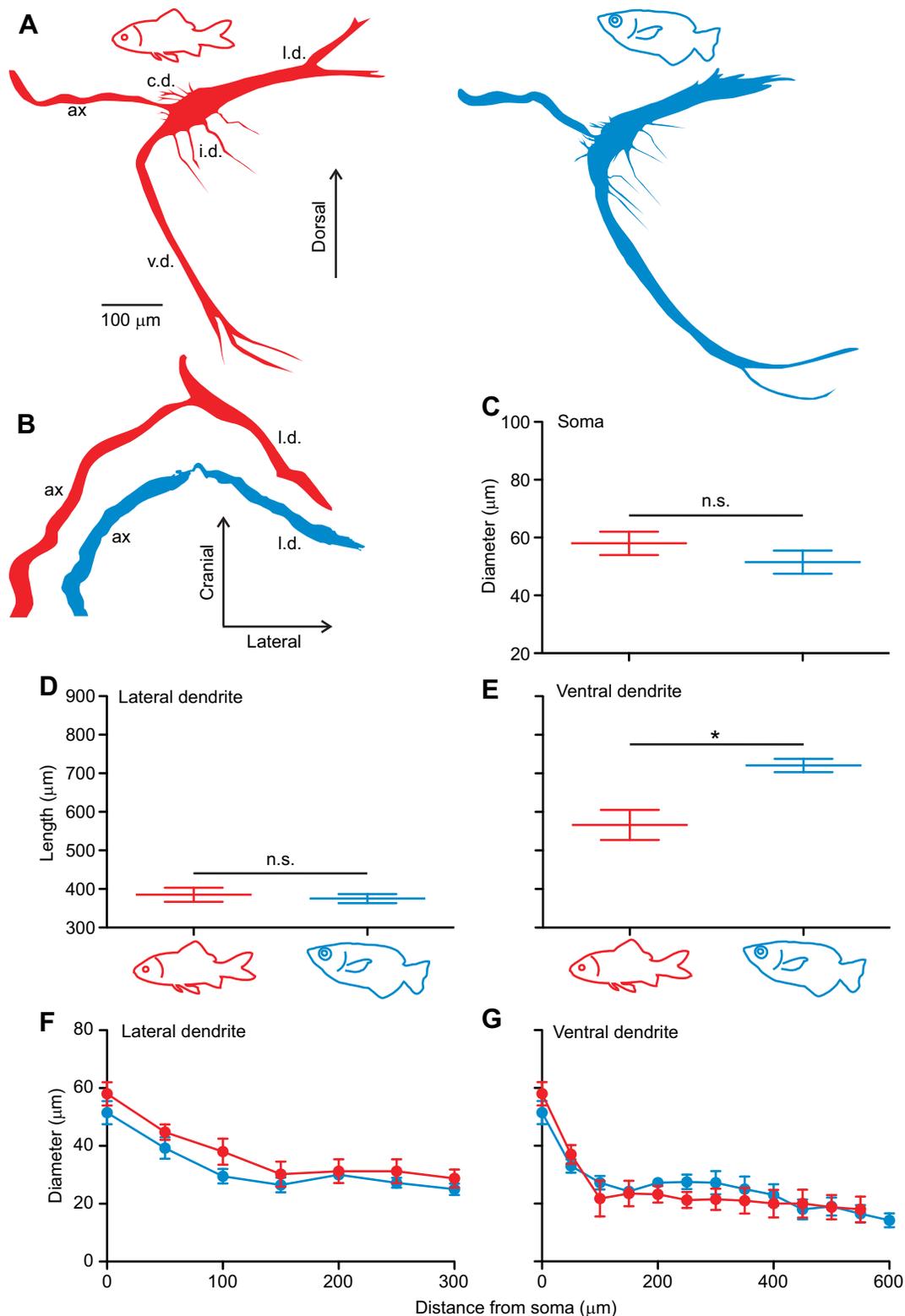
Fig. 5. The archerfish Mauthner cell is remarkably similar to that of equally sized goldfish. (A,B) Partial reconstruction of the goldfish right Mauthner neuron (in red) and a neuron that was penetrated at the focus point in the archerfish right medulla (in blue). The neurons show striking similarities in rough morphology, size and orientation of the lateral (l.d.) and ventral (v.d.) dendrites and both show cap dendrites (c.d.) and inferior dendrites (i.d.). Neurons were reconstructed from coronal (A) or horizontal (B) slices. Note that the ventral dendrite (v.d.) cannot be seen in B because of its orientation. ax, initial part of the axon. (C–G) Comparison of soma diameter (C), length of the lateral dendrite (D), length of the ventral dendrite (E), diameter of the lateral dendrite (F) and diameter of the ventral dendrite (G) of archerfish and goldfish (as indicated) of the same size and with cells stained and processed in the same way. $N=4$ in all diagrams. Data are shown as mean (middle bar/circle) and s.e.m. n.s., not significant; *$P<0.05$.

presence of an all-or-none field potential the latency of which is indistinguishable from that of the candidate Mauthner cell's action potential suggests the presence of a so-called axon cap. To compare the rough morphology of the archerfish Mauthner cell with that of goldfish, six goldfish and six archerfish Mauthner cells were processed and evaluated in the same way, so that we could compare relative sizes. In each species, two brains were sliced horizontally and four brains coronally. Fig. 5 shows reconstructed Mauthner cells of archerfish and goldfish in coronal (Fig. 5A) and horizontal (Fig. 5B) view in the same scale and orientation. Soma cross-sectional diameters were in the range 45–63 µm (52±4 µm; N=4; Fig. 5C) in archerfish and 47–66 µm (58±4 µm; N=4) in goldfish. In all preparations, the archerfish Mauthner cells clearly showed two primary dendrites, smaller inferior dendrites arising from the soma and cap dendrites in the region of the axon hillock (Fig. 5A). The orientation of the primary dendrites in archerfish was as in the goldfish Mauthner cell. One of the primary dendrites of the archerfish Mauthner cell is oriented laterally (lateral dendrite). The horizontal section shows that this dendrite is also oriented slightly caudally from the soma to its distal part (Fig. 5B). The coronal view of the Mauthner neuron (Fig. 5A) indicates that the lateral dendrite is in addition directed upwards from its proximal to its distal part. Short branches are typical for its terminal region. We detected no significant difference in the length of the lateral dendrite between goldfish and archerfish (Fig. 5D), as measured by the distance from the Mauthner axon hillock to the distal branches of the lateral dendrite [Mann–Whitney test, P=0.77; in goldfish: 385±18 µm (N=4); in archerfish: 375±12 µm (N=4)]. However, the goldfish lateral dendrites consistently had a larger diameter (Fig. 5F; Wilcoxon matched-pairs signed rank test, P=0.02). Averaged across the sampling points along the lateral dendrite, its diameter was 33±4 µm (N=4) in archerfish and 37±4 µm (N=4) in goldfish. The second primary dendrite is oriented ventrally (ventral dendrite). The sequence of consecutive coronal slices indicated that the ventral dendrite is also oriented cranially. Its distal part is deeply cleaved and terminates in at least two branches (Fig. 5A). In contrast to the lateral dendrite, the length of the ventral dendrite differed between goldfish and archerfish (Fig. 5E). The distance from the axon hillock to the distal part of the ventral dendrite was significantly larger in archerfish [Mann–Whitney test; P=0.029; goldfish: 566±39 µm (N=4); archerfish: 720±17 µm (N=4)]. However, the diameter of the ventral dendrite did not differ between goldfish and archerfish (Fig. 5G; Wilcoxon matched-pairs signed rank test, P=0.3). Averaged across the sampling points along the ventral dendrite, its diameter was 25±3 µm (N=4) in goldfish and 27±3 µm (N=4) in archerfish. As shown in Fig. 6, the archerfish Mauthner axon crosses the midline just as in goldfish and is located below the ventricle system (i.e. the fourth ventricle or the spinal canal, respectively).

Are there additional Mauthner-like neurons that do not radiate a field potential?

So far, our findings have identified the archerfish Mauthner cell (Fig. 6A), its location in the medulla (Figs 3D,E, 6B) and its striking morphological similarity to that of the goldfish (Fig. 5). However, our findings do not yet exclude two possibilities. First, there could still be an additional system with similarly sized axons to the Mauthner cell (and perhaps similar morphology) that does not radiate a field potential. Second, an additional system – with a similarly large-diameter axon – might even be located outside the medulla. We therefore examined coronal cross-sections of the spinal cord in preparations in which the Mauthner cells had been stained (Fig. 6C) and in unstained preparations (Fig. 6D). This way, we would be able to

discover any additional unstained and yet thick axons corresponding to cells that did not radiate a field potential and/or were located outside the medulla. However, our findings (in four of four archerfish examined) clearly ruled this out. The unstained cross-sections show two and only two axons with outstandingly large diameter (Fig. 6D), extending up to the end of the spinal cord. In every spinal cord slice we made, we could clearly identify them. Moreover, in preparations with stained Mauthner cells (N=4 archerfish), the stained Mauthner axons were the largest ones in the spinal cord and were in similar locations to the largest axons seen in the unstained preparations (Fig. 6C,D). Based on this evidence, we conclude that there are no other neurons that send equally large-diameter axons down the spinal cord – either outside the medulla or ones that do not radiate a field potential. The unstained sections, photographed immediately after slicing under wet conditions, give the most accurate estimate of the actual axonal diameter of the two largest axons: 71.9±3.8 µm (n=10, N=4). When quantified in the same way as in goldfish, the Mauthner cell axonal diameter of archerfish was found to be remarkably similar (73.6±1.7 µm; n=10, N=4 goldfish), but also fitted values reported for goldfish in the literature (e.g. Celio et al., 1979; Funch et al., 1981). Thus, there are two and only two axons of such a diameter, which strikingly exceeds that of any other axon, that coincide with the axons of the labelled Mauthner cells and that have diameters like those of Mauthner axons of similar sized goldfish processed in the same way (Fig. 6E) and in agreement with the literature. This is fully supported by the conduction speed calculated from latency values (Fig. 2) and the known distance from the source of spinal cord stimulation. Conduction speed was 101±1 m s^{-1} (N=30) in archerfish and 101±4 m s^{-1} (N=14) in goldfish. These values are (i) not statistically different between the two species (P=0.9, t-test) and (ii) in accord with published values for goldfish of similar size (Funch et al., 1981).

DISCUSSION

In this study, we have provided unequivocal evidence that the archerfish reticulospinal system includes a pair of teleost-typical Mauthner cells. As in goldfish, the archerfish Mauthner cell can also be located by a signature all-or-none field potential. By directly comparing equally sized goldfish and archerfish we show that the Mauthner cells of the two species are strikingly similar, except for slight differences in the length and diameter of the two major dendrites. Our findings lay the necessary foundation for the dissection of the fast-start system in archerfish and for testing a potential involvement of the archerfish Mauthner cell in the two C-start manoeuvres. They are also the basis for a direct physiological comparison of the archerfish and goldfish Mauthner cell that is reported in the accompanying paper (Machnik et al., 2018). Finally, the outstanding size both of the soma and of the axon diameter of the archerfish Mauthner cell and our finding that these sizes are not significantly different in the Mauthner cells of equally sized goldfish do not support the view (Bhattacharyya et al., 2017) that Mauthner cells should be reduced in species with more flexible fast-start manoeuvres.

Similarities between the Mauthner neurons in archerfish and goldfish

We showed here that a typical field potential accompanies Mauthner cell activation in archerfish, which can be traced back to a single point-like source per medullary hemisphere in the direct vicinity of the Mauthner cell. The decay of the field potential with distance from its centre was remarkably similar in archerfish and goldfish and matches previous findings in goldfish (e.g. Furshpan and Furukawa,
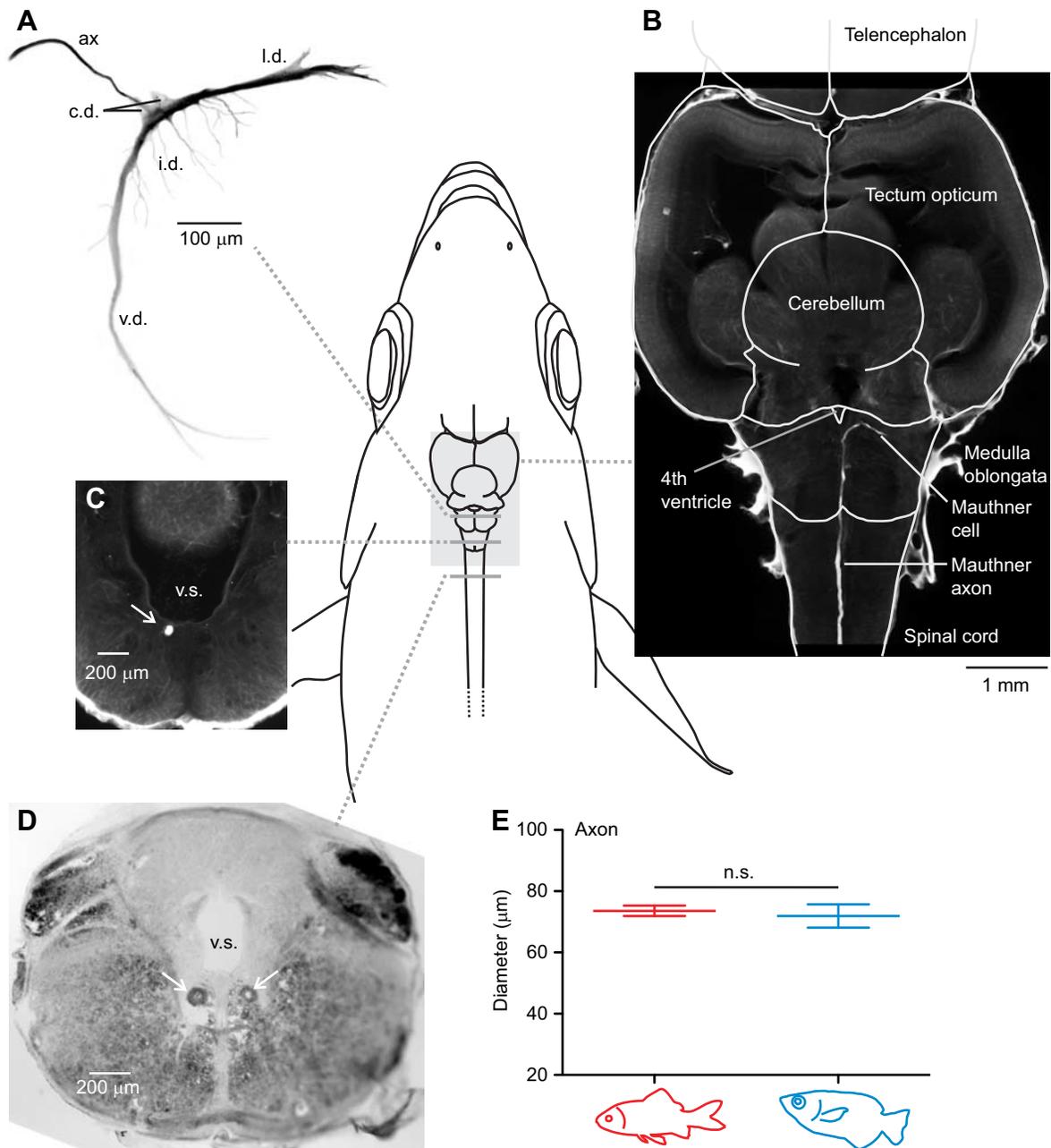
Fig. 6. Evidence against any other neurons with Mauthner-like axon diameters. (A) A more detailed reconstruction of the archerfish Mauthner cell at the focus point in the recordings of Fig. 4. Its large soma and its large lateral (l.d.) and ventral (v.d.) dendrites can be seen as well as additional inferior dendrites (i.d.) and dendrites in the region of the axon hillock (cap dendrites; c.d.). Note also the initial part of the Mauthner axon (ax). (B) The location of the (right) Mauthner cell in the medulla of an archerfish and the point at which its axon crosses the midline to run down the spinal cord on the side contralateral to the cell body. Note that the large ventral dendrite cannot be seen in this horizontal section. (C) Coronal view of the archerfish spinal cord with a stained axon (arrow) of the right Mauthner cell directly below the ventricle system (v.s.). (D) View of the spinal cord directly after slicing under wet conditions showing only two axons (arrows) of by far the largest diameter (of 70 µm diameter), the position and size of which coincide with those of the stained Mauthner axons. (E) The diameter also coincides with that measured in unstained Mauthner axons of similar-sized goldfish. Diameters reported as means±s.e.m. are from unstained neurons of N=4 archerfish and N=4 goldfish. n.s., not significant.

1962; Faber and Korn, 1978). Although the earlier goldfish work used a simple Coulomb potential to model the decay, it is evident that an exponential decay fits the data far better for both archerfish and goldfish. The deviation from a Coulomb potential is likely to be the result of boundary conditions at the surface of the brain, but not to more distributed sources that each has a Coulomb potential. In archerfish, the Mauthner cell is located about 1 mm below the surface of the medulla, slightly closer to the surface than the goldfish

Mauthner cell. However, the search for the archerfish Mauthner cell can similarly be guided by characteristic landmarks in the brain, with remarkably similar patterns of variation in the two species (see Fig. 3D,E). Because we had stained Mauthner cells of goldfish and archerfish of the same size using the same protocols, and because we could compare the goldfish values with values reported in the literature, we feel confident in concluding that the somata and axon diameters of their Mauthner cells are not statistically different and

that the relative length of the ventral dendrites differs, with a longer ventral dendrite in the archerfish Mauthner cell. Moreover, the diameter of the lateral dendrite is slightly larger in goldfish. In goldfish, the ventral dendrite has been shown to receive visual input (Zottoli et al., 1987), whereas the lateral dendrite receives mechanosensory input (e.g. Zottoli and Faber, 1979; Mirjany and Faber, 2011). It is therefore tempting to speculate that the differences in the dendrites may reflect the importance of respective sensory information in the two species.

First implications for the role played by the archerfish Mauthner cell

With a giant and teleost-typical Mauthner cell and an axon diameter that similarly stands out among other reticulospinal neurons as it does in goldfish, it is obvious that the evolution of a variable, fine-tuned and yet high-power C-start has not made the Mauthner cell obsolete in archerfish. Because Mauthner cells in zebrafish larvae were found not to be recruited in slower and more variable C-starts (Bhattacharyya et al., 2017), it was suggested that Mauthner cells generally were not useful for animals with more variable rapid behaviours. At least morphologically, this expectation is clearly not supported by our findings in the archerfish reticulospinal system. However, the advent of the predictive C-starts has also not led to a major re-shaping in the archerfish Mauthner cell: it appears basically just like that of goldfish, with only slight differences in the dendrites. But, a complete picture does require comparison of key physiological and network properties of the archerfish Mauthner neuron and the archerfish Mauthner cell could still functionally be very different from that of goldfish. The accompanying paper (Machnik et al., 2018) therefore will deal with these important aspects.

References

Bhattacharyya, K., McLean, D. L. and MacIver, M. A. (2017). Visual threat assessment and reticulospinal encoding of calibrated responses in larval zebrafish. *Curr. Biol.* **27**, 2751-2762.

Celio, M. R., Gray, E. G. and Yasargil, G. M. (1979). Ultrastructure of the Mauthner axon collateral and its synapses in the goldfish spinal cord. *J. Neurocyt.* **8**, 19-29.

DiDomenico, R., Nissanov, J. and Eaton, R. C. (1988). Lateralization and adaptation of a continuously variable behavior following lesions of a reticulospinal command neuron. *Brain Res.* **473**, 15-28.

Dunn, T. W., Gebhardt, C., Naumann, E. A., Riegler, C., Ahrens, M. B., Engert, F. and Del Bene, F. (2016). Neural circuits underlying visually evoked escapes in larval zebrafish. *Neuron* **89**, 613-628.

Eaton, R. C. (1984). *Neural Mechanisms of Startle Behavior*. New York: Plenum Press.

Eaton, R. C., Lavender, W. A. and Wieland, C. M. (1981). Identification of Mauthner-initiated response patterns in goldfish: evidence from simultaneous cinematography and electrophysiology. *J. Comp. Physiol.* **144**, 521-531.

Eaton, R. C., Lavender, W. A. and Wieland, C. M. (1982). Alternative neural pathways initiate fast-start responses following lesions of the Mauthner neuron in goldfish. *J. Comp. Physiol.* **145**, 485-496.

Eaton, R. C., Hofve, J. C. and Fetcho, J. R. (1995). Beating the competition: the reliability hypothesis for Mauthner axon size. *Brain Behav. Evol.* **45**, 183-194.

Faber, D. S. and Korn, H. (1978). Electrophysiology of the Mauthner cell: basic properties, synaptic mechanisms, and associated networks. In *Neurobiology of the Mauthner Cell* (ed. D. S. Faber and H. Korn), pp. 47-131. New York: Raven Press.

Faber, D. S., Fetcho, J. R. and Korn, H. (1989). Neuronal networks underlying the escape response in goldfish. *Ann. N. Y. Acad. Sci.* **563**, 11-33.

Fetcho, J. R. (1991). Spinal network of the Mauthner cell. *Brain Behav. Evol.* **37**, 298-316.

Fetcho, J. R. (1992). Excitation of motoneurons by the Mauthner axon in goldfish: complexities in a "simple" reticulospinal pathway. *J. Neurophysiol.* **67**, 1574-1586.

Foreman, M. B. and Eaton, R. C. (1993). The direction change concept for reticulospinal control of goldfish escape. *J. Neurosci.* **13**, 4101-4113.

Funch, P. G., Kinsman, S. L., Faber, D. S., Koenig, E. and Zottoli, S. J. (1981). Mauthner axon diameter and impulse conduction velocity decrease with growth of goldfish. *Neurosci. Lett.* **27**, 159-164.

Furshpan, E. J. and Furukawa, T. (1962). Intracellular and extracellular responses of the several regions of the Mauthner cell of the goldfish. *J. Neurophysiol.* **25**, 732-771.

Huang, Q., Zhou, D. and DiFiglia, M. (1992). Neurobiotin™, a useful neuroanatomical tracer for in vivo anterograde, retrograde and transneuronal tract-tracing and for in vitro labeling of neurons. *J. Neurosci. Meth.* **41**, 31-43.

Kimmel, C. B., Eaton, R. C. and Powell, S. L. (1980). Decreased fast-start performance of zebrafish larvae lacking Mauthner neurons. *J. Comp. Physiol.* **140**, 343-350.

Kohashi, T. and Oda, Y. (2008). Initiation of Mauthner- or non-Mauthner-mediated fast escape evoked by different modes of sensory input. *J. Neurosci.* **28**, 10641-10653.

Korn, H. and Faber, D. S. (1996). Escape behavior – brainstem and spinal cord circuitry and function. *Curr. Opin. Neurobiol.* **6**, 826-832.

Korn, H. and Faber, D. S. (2005). The Mauthner cell half a century later: a neurobiological model for decision-making? *Neuron* **47**, 13-28.

Liu, K. S. and Fetcho, J. R. (1999). Laser ablations reveal functional relationships of segmental hindbrain neurons in zebrafish. *Neuron* **23**, 325-335.

Machnik, P., Leupolz, K., Feyl, S., Schulze, W. and Schuster, S. (2018). The Mauthner cell in a fish with top-performance and yet flexibly-tuned C-starts. II. Physiology. *J. Exp. Biol.* **221**, jeb175588.

Mirjany, M. and Faber, D. S. (2011). Characteristics of the anterior lateral line nerve input to the Mauthner cell. *J. Exp. Biol.* **214**, 3368-3377.

Neki, D., Nakayama, H., Fujii, T., Matsui-Furusho, H. and Oda, Y. (2014). Functional motifs composed of morphologically homologous neurons repeated in the hindbrain segments. *J. Neurosci.* **34**, 3291-3302.

Neumeister, H., Szabo, T. M. and Preuss, T. (2008). Behavioral and physiological characterization of sensorimotor gating in the goldfish startle response. *J. Neurophysiol.* **99**, 1493-1502.

Oda, Y., Kawasaki, K., Morita, M., Korn, H. and Matsui, H. (1998). Inhibitory long-term potentiation underlies auditory conditioning of goldfish escape behaviour. *Nature* **394**, 182-185.

Preuss, T. and Faber, D. S. (2003). Central cellular mechanisms underlying temperature-dependent changes in the goldfish startle-escape behavior. *J. Neurosci.* **23**, 5617-5626.

Preuss, T., Osei-Bonsu, E., Weiss, S. A., Wang, C. and Faber, D. S. (2006). Neural representation of object approach in a decision-making motor circuit. *J. Neurosci.* **26**, 3454-3464.

Reinel, C. and Schuster, S. (2014). Pre-start timing information is used to set final linear speed in a C-start manoeuvre. *J. Exp. Biol.* **217**, 2866-2875.

Reinel, C. P. and Schuster, S. (2016). Archerfish fast-start decisions can take an additional variable into account. *J. Exp. Biol.* **219**, 2844-2855.

Rischawy, I., Blum, M. and Schuster, S. (2015). Competition drives sophisticated hunting skills of archerfish in the wild. *Curr. Biol.* **25**, R595-R597.

Rossel, S., Corlija, J. and Schuster, S. (2002). Predicting three-dimensional target motion: how archer fish determine where to catch their dislodged prey. *J. Exp. Biol.* **205**, 3321-3326.

Schlegel, T. and Schuster, S. (2008). Small circuits for large tasks: high-speed decision-making in archerfish. *Science* **319**, 104-106.

Sillar, K. T. (2009). Mauthner cells. *Curr. Biol.* **19**, R353-R355.

Sillar, K. T., Picton, L. D. and Heitler, W. J. (2016). *The Neuroethology of Predation and Escape*. Oxford, Chichester, New York: Wiley Blackwell.

Smith, M. and Pereda, A. E. (2003). Chemical synaptic activity modulates nearby electrical synapses. *Proc. Natl. Acad. Sci. USA* **100**, 4849-4854.

Stefanelli, A. (1951). The Mauthnerian apparatus in the Ichthyopsida: its nature and function and correlated problems of neurohistogenesis. *Q. Rev. Biol.* **26**, 17-34.

Stefanelli, A. (1980). I neuroni di Mauthner degli Ittiopside. Valutazioni comparative morfologiche e funzionali. *Att. Accad. Naz. Lincei Mem. Cl. Sci. Fis. Mat. Nat. Sez. III, Series 8* **16**, 1-45.

Szabo, T. M., Brookings, T., Preuss, T. and Faber, D. S. (2008). Effects of temperature acclimation on a central neural circuit and its behavioral output. *J. Neurophysiol.* **100**, 2997-3008.

Wöhl, S. and Schuster, S. (2006). Hunting archer fish match their take-off speed to distance from the future point of catch. *J. Exp. Biol.* **209**, 141-151.

Wöhl, S. and Schuster, S. (2007). The predictive start of hunting archer fish: a flexible and precise motor pattern performed with the kinematics of an escape C-start. *J. Exp. Biol.* **210**, 311-324.

Zottoli, S. J. (1977). Correlation of the startle reflex and Mauthner cell auditory responses in unrestrained goldfish. *J. Exp. Biol.* **66**, 243-254.

Zottoli, S. J. (1978). Comparative morphology of the Mauthner cell in fish and amphibians. In *Neurobiology of the Mauthner cell* (ed. D. S. Faber and H. Korn), pp. 13-45. New York: Raven Press.

Zottoli, S. J. and Faber, D. S. (1979). Properties and distribution of anterior VIIIth nerve excitatory inputs to the goldfish Mauthner cell. *Brain Res.* **174**, 319-323.

Zottoli, S. J. and Faber, D. S. (2000). The Mauthner cell: what has it taught us? *Neuroscientist* **6**, 26-38.

Zottoli, S. J., Hordes, A. R. and Faber, D. S. (1987). Localization of optic tectal input to the ventral dendrite of the goldfish Mauthner cell. *Brain Res.* **401**, 113-121.

Zottoli, S. J., Newman, B. C., Rieff, H. I. and Winters, D. C. (1999). Decrease in occurrence of fast startle responses after selective Mauthner cell ablation in goldfish (*Carassius auratus*). *J. Comp. Physiol. A* **184**, 207-218.